Radiotherapy and Oncology 140 (2019) 98–104

Contents lists available at ScienceDirect

Radiotherapy and Oncology

journal homepage: www.thegreenjournal.com

Original Article

# Liver phantom design and dosimetric verification in participating institutions for a proton beam therapy in patients with resectable hepatocellular carcinoma: Japan Clinical Oncology Group trial (JCOG1315C)

Teiji Nishio [a,*], Hidenobu Tachibana [b], Yuki Kase [c], Kenji Hotta [b], Mitsuhiro Nakamura [d], Masaya Tamura [e], Toshiyuki Terunuma [f], Toshiyuki Toshito [g], Haruo Yamashita [c], Satoshi Ishikura [h], Hiroshi Fuji [i], Tetsuo Akimoto [b], Yasumasa Nishimura [j]

[a] *Department of Medical Physics, Graduate School of Medicine, Tokyo Women's Medical University;* [b] *Division of Radiation Oncology and Particle Therapy, Exploratory Oncology Research and Clinical Trial Center, National Cancer Center, Kashiwa;* [c] *Proton Therapy Division, Shizuoka Cancer Center Research Institute;* [d] *Division of Medical Physics, Department of Information Technology and Medical Engineering, Human Health Sciences, Graduate School of Medicine, Kyoto University;* [e] *Department of Medical Physics, Hokkaido University Hospital, Sapporo;* [f] *Faculty of Medicine, University of Tsukuba;* [g] *Department of Proton Therapy Physics, Nagoya Proton Therapy Center, Nagoya City West Medical Center;* [h] *Department of Radiology, Graduate School of Medical Sciences, Nagoya City University;* [i] *Department of Radiation Oncology, National Center for Child Health and Development, Tokyo; and* [j] *Department of Radiation Oncology, Kindai University Faculty of Medicine, Osaka-Sayama, Japan*

A R T I C L E  I N F O

*Article history:*
Received 26 September 2018
Received in revised form 15 May 2019
Accepted 5 June 2019
Available online 29 June 2019

*Keywords:*
Dosimetric verification
Water tank-type liver phantom
Liver proton therapy clinical trial

A B S T R A C T

*Background and purpose:* In Japan, the first domestic clinical trial of proton beam therapy for the liver was initiated as the Japan Clinical Oncology Group trial (JCOG1315C: Non-randomized controlled study comparing proton beam therapy and hepatectomy for resectable hepatocellular carcinoma). Purposes of this study were to develop a new dosimetric verification system and to carry out a credentialing for the JCOG1315C clinical trial.

*Materials and methods:* Accuracy and differences in doses in proton treatment planning among participating institutions were surveyed and investigated. We designed and developed a suitable water tank-type liver phantom for a dosimetric verification of proton beam therapy for liver. In a visiting survey of five institutions participating in the clinical trial, we performed the dosimetric verification using the liver phantom and an air-filled ionization chamber.

*Results:* The shape of the dose distributions calculated in proton treatment planning was characteristic and dependent on the manufacturers of the proton beam therapy system, the proton treatment planning system and the setup at the participating institutions. Widths of the lateral penumbra were 5.8–12.7 mm among participating institutions. The accuracy between the calculated and the measured doses in the proton irradiation was within 3% at five measurement points including both points on the isocenter and off the isocenter.

*Conclusions:* These findings confirmed the accuracy of the delivery doses in the institutions participating in the clinical trial, and the clinical trial with integration of all institutions (five institutions) could be initiated.



In proton beam therapy, irradiation dose can be concentrated on a tumor by modulation and optimization of the radiation dose peak, known as the Bragg Peak [1–4]. Recently, proton beam therapy with high precision and safety for patients has become possible by the use of various innovative technologies. Furthermore, the number of proton beam therapy facilities and systems has been increasing world-wide [5].

Broad beam irradiation and pencil beam scanning methods are used for the clinical proton dose distribution [4]. In a broad beam irradiation method, a uniform dose distribution is obtained with a field dose by a dual-ring double scattering method or a wobbling method, and the depth dose distribution of the spread-out Bragg Peak (SOBP) is obtained with a bar ridge filter or a range modulator wheel. The dose distribution is fitted to the tumor shape in each patient and it is adjusted with a patient compensator and collima-

* Corresponding author at: Department of Medical Physics, Graduate School of Medicine, Tokyo Women's Medical University, 8-1, Kawada-cho, Shinjuku-ku, Tokyo 162-8666, Japan.
*E-mail address:* nishio.teiji@twmu.ac.jp (T. Nishio).

https://doi.org/10.1016/j.radonc.2019.06.005
0167-8140/

tor or a multi leaf collimator (MLC) mounted on the beam irradiation nozzle. In a pencil beam scanning method, the dose distribution in each patient is provided by a spot or raster beam scanning method [6,7]. Furthermore, intensity-modulated proton therapy (IMPT) [8,9] is carried out using the pencil beam scanning technique. The proton beam irradiation method differs for each of the proton beam therapy system manufacturers. Therefore, shape of the dose distribution and beam quality differ for each institution, and control of the proton dose irradiated onto a tumor and organ at risk (OAR) among institutions is required in multi-institutional clinical trials of proton beam therapy.

The Imaging and Radiation Oncology Core (IROC) Houston Quality Assurance (QA) Center pioneered a credentialing program of quality assurance for clinical trials of proton beam therapy [10,11]. In Japan, multi-institutional clinical trials of radiotherapy have been conducted by the Radiation Therapy Study Group (RTSG) of the Japan Clinical Oncology Group (JCOG) [12]. The Medical Physics Working Group (MPWG) of the JCOG/RTSG has been conducting dosimetry credentialing for the JCOG radiotherapy trials as its main mission [13–19]. Although 16 proton therapy facilities are in operation in Japan, multi-institutional clinical trials have not, so far, been implemented.

The first domestic clinical trial in Japan of proton beam therapy for the liver was initiated as the JCOG trial, JCOG1315C (Non-randomized controlled study comparing proton beam therapy and hepatectomy for resectable hepatocellular carcinoma; UMIN000027811 [20]). The purpose of this study is to develop a new dosimetric verification system for a liver proton beam therapy based on the many verification systems that we have already developed for previous JCOG radiotherapy trials [12–18]. Various physical verifications such as accuracy of dose, beam range, tumor position, tumor motion, and so on, were required for the credentialing of JCOG1315C clinical trial. We thought that it was important to know the characteristics of the basic proton beam used at each facility. Therefore, in this study, we focused on dose verification first. Taylor et al. [10] reported a study using radiochromic film and TLD in an anthropomorphic phantom for credentialing of a proton beam therapy clinical trial. In our preliminary verification and in two other reports [21,22], we found that the proton dose measured with radiochromic film has a strong dependence on stopping power of the proton beam, which is ≥0.67 MeV/mm (residual energy ≤ 35.8 MeV, residual range ≤ 12.8 mmWEL). Also, a glass dosimeter has been used for a postal dose audit of high-energy radiotherapy photon beams in Japan [18,23,24]. However, studies on the characteristics of proton dose of the glass dosimeter are insufficient. Therefore, in this study, we used only an air-filled ionization chamber was used for dose measurement and verification for the credentialing of the JCOG1315C clinical trial by making a visiting survey of all participating institutions.

## Materials and methods

### *Design of water tank type phantom for dosimetric verification of liver proton beam therapy*

We designed a water tank-type phantom for dosimetric verification of liver proton beam therapy based on technology of the lung phantom developed for a lung stereotactic body radiotherapy [14]. Fig. 1 has photos of the phantom for dosimetric verification of proton beam therapy and its parts. This liver phantom is comprised

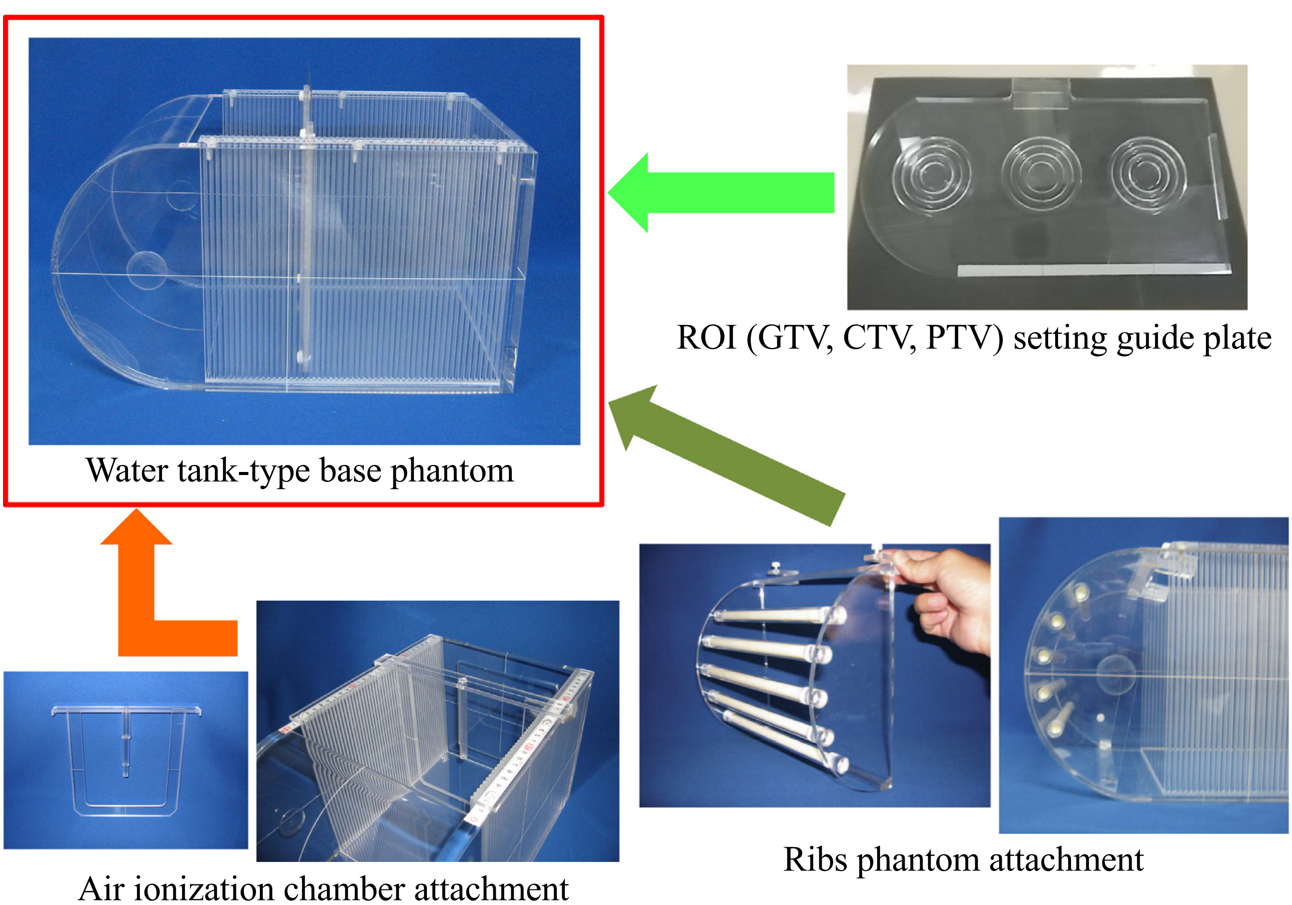


**Fig. 1.** Photos of the water tank type phantom for dosimetric verification of proton beam therapy.

of a water tank made of a thin acryl plate (thickness, 3 mm). The plate through which the beam passes is formed in a rectangular shape having one curved side with a radius of 8 cm. The phantom has the following dimensions: 40 cm (right-left) width and 22 cm (anterior-posterior) length in an axial plane, and 24.5 cm (head-feet) length in the longitudinal direction. We designed a bone equivalent sub-phantom tool of ribs (BE-H (element composition, H:C:N:O:P:Cl:Ca = 0.051:0.425:0.017:0.281:0.070:0.001:0.155; mass density, 1.50 g/cm$^3$; effective atomic number, 11.70; relative stopping power ratio, 1.43), Kyoto Kagaku Co. Ltd., Kyoto, Japan) for dosimetric verification in liver proton beam therapy, and this tool can be installed in the water tank phantom. Furthermore, attachments for dose measurement with an air-filled ionization chamber can be inserted in the water tank phantom, making dosimetric verification of high flexibility possible. In treatment planning of proton beam therapy, regions-of-interest (ROIs) of the gross tumor volume (GTV), clinical target volume (CTV) and planning target volume (PTV) are drawn and inputted at the prescribed position on a computed tomography (CT) image by use of the ROI guide setting plate. In addition, the water tank type phantom is suitable for use in visiting and postal surveys for dosimetric verification because the phantom weight is approximately 2 kg after draining out the water.

### *Information describing the irradiation system, device, and irradiation method at each institution*

We visited all institutions (five institutions) participating in the JCOG1315C clinical trial for the dosimetric survey which was performed using the liver phantom designed for proton beam therapy. Dose distribution calculated in the proton treatment planning and measured absolute dose were verified and compared among the five institutions. The dosimetric verification tools of the water tank-type liver phantom, air-filled ionization chamber (3D PinPoint chamber (31016), PTW GmbH, Freiburg, Germany), and electrometer (UNIDOS webline, PTW GmbH, Freiburg, Germany) were sent using the postal service to the selected institutions prior to our visit. Dose calibration of the 3D PinPoint chamber was performed by the cross-calibration method with an air-filled ionization chamber of the Farmer type (Farmer chamber (30013), PTW GmbH, Freiburg, Germany) with therapeutic proton beam. Absolute dose of the Farmer chamber was calibrated by the protocol of the Standard Dosimetry 12 of the Japan Society of Medical Physics [25], which recommended an arrangement for Japanese institutions from the TRS 398 report of the International Atomic Energy Agency [26].

In the JCOG1315C clinical trial, five types of proton beam therapy systems were surveyed: Proton Therapy System (C235) manufactured by Sumitomo Heavy Industries, PROBEAT, PROBEAT III and PROBEAT-RT manufactured by Hitachi, and Proton Therapy System (Proton Type) manufactured by Mitsubishi Electric. Three types of proton treatment planning system were used: ptplan manufactured by Sumitomo Heavy Industries, VQA manufactured by Hitachi, and XiO-M manufactured by ELEKTA. The therapeutic proton beam accelerator was the cyclotron type in one institution and the synchrotron type in the other four institutions. Methods of therapeutic proton beam irradiation were broad beam irradiation in four institutions (dual-ring double scattering method in three institutions and a wobbling method in one institution) and spot scanning irradiation in one institution. Depth dose distribution of the SOBP for the broad beam irradiation was formed with a bar ridge filter in three institutions and a range modulator wheel in one institution. Three types of respiratory gating systems were used for control of beam irradiation in liver proton beam therapy [27,28]: AZ-733 V (Anzai Medical) in three institutions; an in-house laser rangefinder (University of Tsukuba) in one institution; and Real Time Tumor-tracking System (Hitachi) in one institution. These are summarized in Table 1.

### *Procedure of dosimetric verification for liver proton beam therapy*

Fig. 2(a) shows a photo of the CT imaging setup with the phantom for liver proton beam therapy. The CT slice thickness was less than 4 mm. In the proton treatment planning, ROI of the spherical target (GTV) with a 5 cm diameter was drawn at a depth point of 8 cm from the body surface of the phantom on the CT image (Fig. 2(b)). ROI of the CTV was expanded with a three-dimensional auto 10-mm margin from the ROI of the GTV. ROI of the ITV was expanded with a 3–5 mm margin in the direction of the head-feet axis from the ROI of CTV, and ROI of the PTV was generated by expansion of a three-dimensional auto 5-mm margin of the ROI of ITV.

The treatment planning and the dose calculation were performed by one-port proton beam irradiation of 270-degree gantry angle to the PTV (Fig. 2(b)). The proton dose was calculated by a pencil beam calculation algorithm with calculation grid size of 2 mm. The planned dose was 200.0 cGy or 181.8 cGy (200.0 cGyE (equivalent) with RBE (relative biological effectiveness) = 1.1) at the PTV center, which was matched with the radiation isocenter. The calibration of the dose monitor of the proton therapy system was carried out using the air-filled ionization chamber owned by each institution. In the broad beam irradiation, the patient compensator and collimator were prepared for each patient and irradiation field (Fig. 2(c)). The results of those treatment planning are summarized in Table 1.

The proton beam defined in the treatment planning was irradiated to the liver phantom. The 3D PinPoint chamber was located at the radiation isocenter (Fig. 2(d)), and the irradiated dose was measured by use of the 3D PinPoint chamber and UNIDOS webline electrometer (Fig. 2(e)). The doses at 17 lateral points including the isocenter and off the isocenter at the depth of the SOBP center in the liver phantom were measured by moving the treatment bed in the direction of the head-feet. The dose measurement points were 0 (radiation isocenter), ±20, ±35, ±40, ±45, ±50, ±55, ±60 and ±65 mm (Fig. 2(f)). We evaluated whether accuracy between the calculated and the measured doses in the proton irradiation plan was within 3% in the 80% full width at half maximum (FWHM) of the off-center ratio (OCR) at the depth of the SOBP center. The measured FWHM was obtained from the distance between the 50% dose levels and measured lateral penumbra using distances between 20% and 80% dose levels in the lateral penumbra region. These values were determined by linear interpolation of the measured dose with a 5 mm step. Accuracy of the measured FWHM and the measured lateral penumbra determined by the linear interpolation was estimated to be a few mm.

## Results

### *Evaluation of planned dose distribution in liver phantom*

Supplementary Fig. 1 shows results at each institution of the planned dose distribution with the 270-degree irradiation angle in the liver phantom. Table 1 summarizes the proton treatment planning in the liver phantom at each institution.

Fig. 3(a) plots results at each institution of the planned percentage depth dose (PDD) normalized at the radiation isocenter and the value of distal fall-off, *P*(80–20), which is the penumbra width between the 80% and 20% doses. The clinical proton beam range at the distal depth of the 94% dose [29] ranged from 41.1 mm water equivalent length (WEL) to 44.6 mmWEL. The clinical SOBP width of distal and proximal 94% doses [29] ranged from 88.8 to 94.8 mmWEL at each institution, and the dose uniformity in the

**Table 1**
Information describing the proton beam therapy system, treatment planning system, proton beam irradiation method specifications as the lateral field and SOBP, respiratory gating system, and proton treatment planning in liver phantom at each institution.

| Institution | | A | B | C 1 | C 2 | D | E |
|---|---|---|---|---|---|---|---|
| Proton Therapy System | | Proton Therapy System (C235)/ Sumitomo Heavy Industries | PROBEAT III/ Hitachi | Particle Therapy System (Proton Type)/Mitsubishi Electric | | PROBEAT/ Hitachi | PROBEAT-RT/Hitachi |
| Proton Accelerator Type | | Cyclotron | Synchrotron | Synchrotron | | Synchrotron | Synchrotron |
| Proton Beam Irradiation Method | | Broad Beam | Broad Beam | Broad Beam | | Broad Beam | Scanning Beam |
| Lateral Field | | Double Scatters | Double Scatters | Wobbler | | Double Scatters | Spot Scanning |
| SOBP | | Bar Ridge Filter | Rotating Modulator Wheel | Bar Ridge Filter | | Bar Ridge Filter | Energy Layer |
| Respiratory Gated Proton Beam Control System | | AZ-733V/Anzai Medical | AZ-733V/ Anzai Medical | AZ-733V/Anzai Medical | | Laser Rangefinder/In House) | Real Time Tumor-tracking System/ Hitachi |
| Treatment Planning System | | ptplan/Sumitomo Heavy Industries | VQA/Hitachi | VQA/ Hitachi | XiO-M/ ELEKTA | VQA/Hitachi | VQA/Hitachi |
| Planning results for dosimetric verification | Plan dose [cGy] | 181.8 | 200.0 | 181.8 | 200.0 | 200.0 | 200.0 |
| | CT slice thickness [mm] | 4.0 | 2.0 | 2.0 | | 1.25 | 2.5 |
| | Dose calculation grid size [mm] | 2.0 | 2.0 | 2.0 | 2.0 | 2.0 | 2.0 |
| | Irradiation Energy [MeV] | 190.0 | 160.0 | 150.0 | 190.0 | 200.0 | 83.6–144.1 |
| | Proton Range [mmWEL] | 175.7 | 134.0 | 132.0 | 208.0 | 211.5 | 54.2–145.7 |
| | SOBP [mmWEL] | 80 | 90 | 90 | 90 | 80 | 80 |
| | Range Shifter [mmWEL] | 41.8 | 3.0 | 0.0 | 77.5 | 68.0 | none |
| | Bolus | Patient Bolus | Patient Bolus | Patient Bolus | | Patient Bolus | none |
| | Aperture | Patient Collimator | Multi Leaf Collimator | Patient Collimator | | Patient Collimator | none |
| | Distance: IC-beam focus [mm] | 2974 | 2626 | X:3057, Y:2671 | | 2596 | X:1350, Y:1925 |
| | Distance: IC-Bolus [mm] | 257 | 139 | 284 | | 316 | none |
| | Distance: IC-Aperture [mm] | 197 | 259 | 213 | | 259 | none |

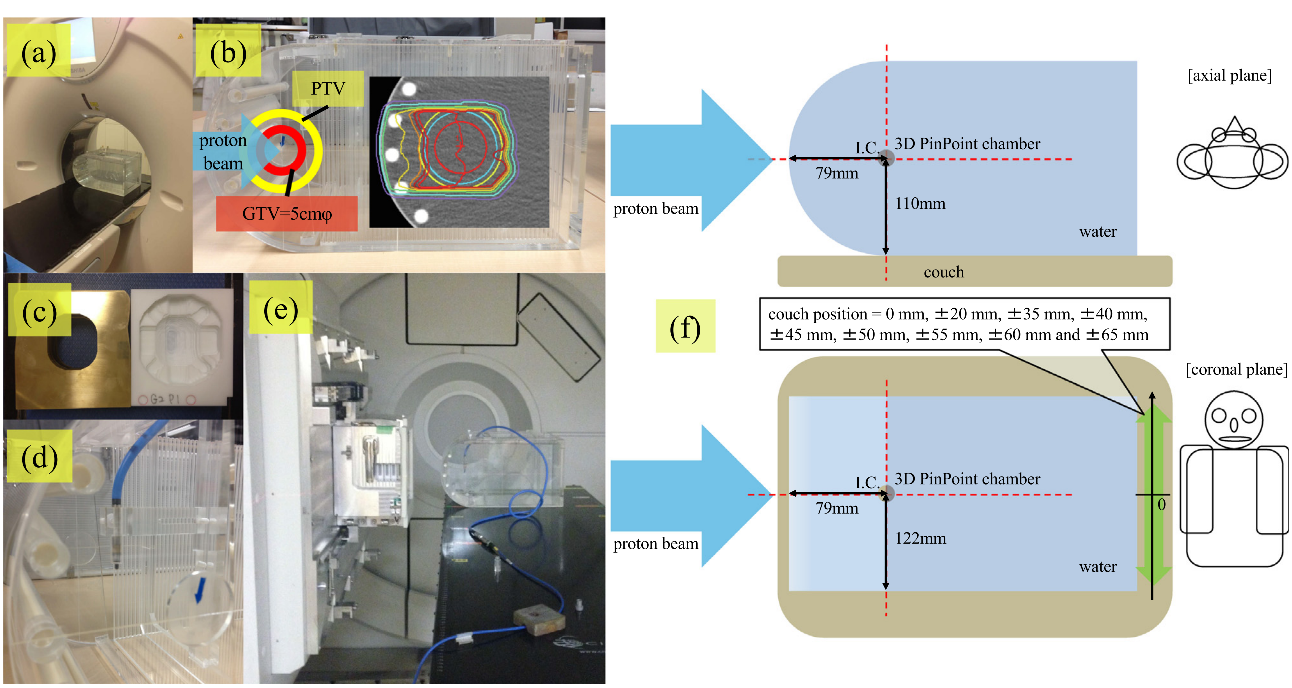


**Fig. 2.** Photos of CT imaging setup (a), irradiation plan setting (b), patient bolus and aperture (c), 3D PinPoint air-filled ionization chamber setting (d), proton irradiation to the liver phantom (e) and setup of proton irradiation (f).

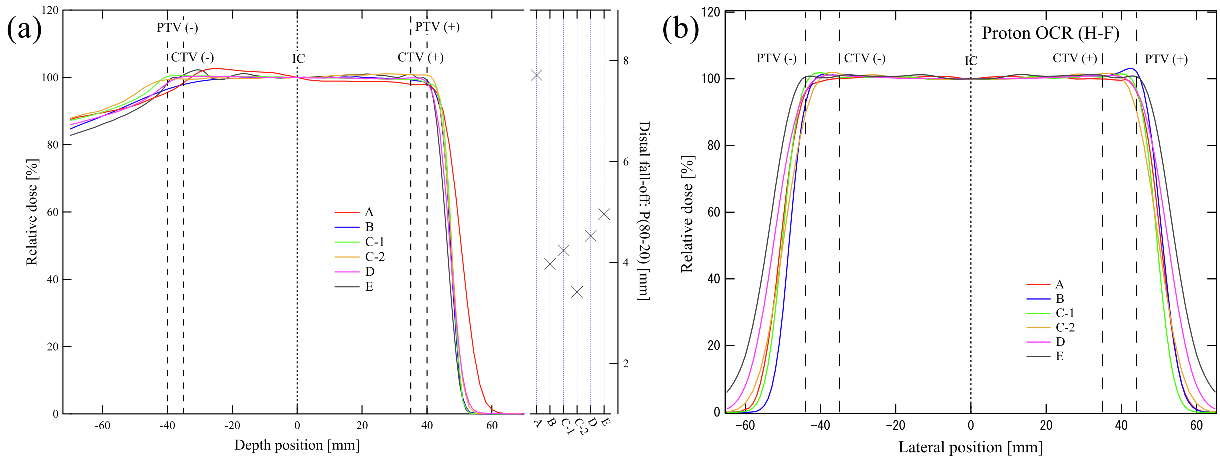


**Fig. 3.** Results at each institution. Planned PDD and distal fall-off of SOBP beam (a) and OCR at SOBP center (b).

clinical SOBP was within 3.5%. The values of distal fall-off were 7.7 mm at one institution and ranged from 3.4 to 5.0 mm at the other institutions. Fig. 3(b) is the planned OCR at the depth of the SOBP center. The dose uniformity in width of the 80% FWHM of the OCR was within ±1.0% at all institutions.

### *Evaluation of measured dose at each position in liver phantom*

Calculated dose obtained with the proton treatment planning system and measured dose obtained with the 3D PinPoint chamber at points on the OCR in the liver phantom are shown for each institution in Fig. 4(a). There was a difference between calculated and measured doses. Counts of the proton beam irradiation monitor were calibrated by the air-filled ionization chamber used for proton beam therapy at each institution. The difference between calculated and measured doses was large in the region of the lateral penumbra in the OCR. Table 2 summarizes the calculated dose, measured dose and dose difference at five lateral positions of 0, ±20, ±35 mm on OCR, which was within the CTV area. In all participating institutions, the dose difference was within 3%, and average of the dose difference was 0(±1)%.

Fig. 4(b) shows the calculated FWHM, the measured FWHM and the difference of these FWHMs. The minimum and maximum values of the FWHM were 99.0 mm and 108.6 mm, respectively. The

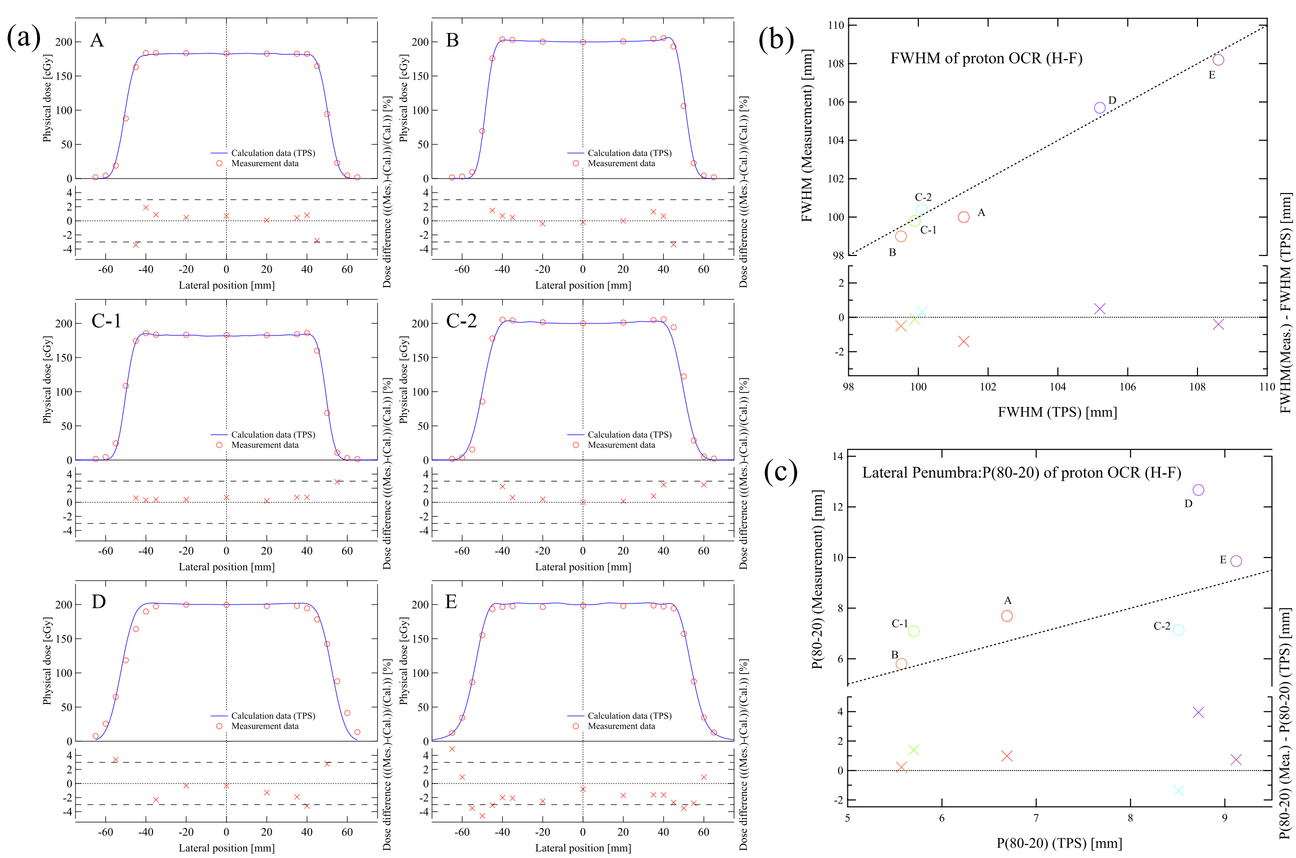


**Fig. 4.** Graphs of calculated and measured doses on OCR in the liver phantom (a), differences between calculated and measured FWHMs (b), and the lateral penumbra (c) at each lateral position.

**Table 2**
Summary of planned and measured doses at lateral positions of 0, ±20 and ± 35 mm.

| Institution | | | Lateral position [mm] | | | | |
|---|---|---|---|---|---|---|---|
| | | | 0 | 20 | −20 | 35 | −35 |
| A | | Planned Dose [cGy]: $D_C$ | 181.8 | 182.7 | 182.5 | 181.8 | 182.1 |
| | | Measured Dose [cGy]: $D_M$ | 183.1 | 182.9 | 183.4 | 182.6 | 183.7 |
| | | Dose Diff. [%]: $(D_M-D_C)/D_C$ | 0.7 | 0.1 | 0.5 | 0.4 | 0.9 |
| B | | Planned Dose [cGy]: $D_C$ | 200.0 | 200.8 | 201.2 | 201.8 | 202.0 |
| | | Measured Dose [cGy]: $D_M$ | 199.5 | 200.8 | 200.4 | 204.5 | 202.9 |
| | | Dose Diff. [%]: $(D_M-D_C)/D_C$ | −0.2 | 0.0 | −0.4 | 1.3 | 0.5 |
| C | 1 | Planned Dose [cGy]: $D_C$ | 181.8 | 182.4 | 182.5 | 182.8 | 182.7 |
| | | Measured Dose [cGy]: $D_M$ | 183.0 | 182.7 | 183.2 | 184.1 | 183.4 |
| | | Dose Diff. [%]: $(D_M-D_C)/D_C$ | 0.7 | 0.2 | 0.4 | 0.7 | 0.4 |
| | 2 | Planned Dose [cGy]: $D_C$ | 200.0 | 200.9 | 200.8 | 203.0 | 203.1 |
| | | Measured Dose [cGy]: $D_M$ | 200.0 | 201.2 | 201.7 | 204.9 | 204.5 |
| | | Dose Diff. [%]: $(D_M-D_C)/D_C$ | 0.0 | 0.2 | 0.4 | 0.9 | 0.7 |
| D | | Planned Dose [cGy]: $D_C$ | 200.0 | 200.6 | 200.5 | 201.9 | 202.1 |
| | | Measured Dose [cGy]: $D_M$ | 199.4 | 197.8 | 199.8 | 198.1 | 197.4 |
| | | Dose Diff. [%]: $(D_M-D_C)/D_C$ | −0.3 | −1.3 | −0.3 | −1.9 | −2.3 |
| E | | Planned Dose [cGy]: $D_C$ | 199.9 | 201.5 | 201.5 | 202.0 | 201.9 |
| | | Measured Dose [cGy]: $D_M$ | 198.4 | 198.0 | 196.5 | 198.6 | 197.7 |
| | | Dose Diff. [%]: $(D_M-D_C)/D_C$ | −0.8 | −1.7 | −2.5 | −1.6 | −2.1 |

difference between planned and measured FWHMs was about 1.5 mm at one institution, and was within 1.0 mm at the other institutions. Fig. 4(c) shows the calculated lateral penumbra, the measured lateral penumbra and the difference of these lateral penumbras. The width of the lateral penumbra ranged from 5.8 mm to 12.7 mm at each institution. The difference between planned and measured lateral penumbras was about 4.0 mm at one institution, and was within 1.5 mm at the other institutions.

## Discussion

For credentialing of the multicenter clinical trial of liver proton beam therapy in JCOG1315C, we performed the evaluation and the verification of proton irradiation dose by the visiting survey to the five participating institutions.

The shape of the proton dose distribution was characteristic and dependent on the manufacturer of in each institution's proton beam therapy system. The distal fall-off of the Bragg peak of the proton beam provided from the cyclotron accelerator was larger than the distal fall-off of proton beam from the synchrotron accelerator. In proton beam therapy, the fixed proton beam energy of the cyclotron accelerator is adjusted and controlled by the energy degrader system. Therefore, deterioration of the distal fall-off of the Bragg peak is thought to occur by the effect of proton-beam momentum spread or energy spread.

The proton beam irradiation with two or three fields is generally used in standard proton beam therapy for liver. From a theoretical viewpoint, the dose uncertainty of proton beam irradiation will be reduced in the region of distal fall-off and the lateral penumbra of the dose distribution, in which the gradient and the change of dose distribution are large. Also, accuracy of the dose calculation with the pencil beam calculation algorithm will be assured in proton beam therapy for liver because the elemental composition of liver is homogeneous. However, the accuracy will deteriorate in the diaphragm region where it is heterogeneous. In this study, the dosimetric verification of the participating institutions was performed by the proton beam irradiation with a single field to get information on the characteristics of the basic proton beam used at each facility. In the broad beam irradiation method in Japan, the dose uniformity of the SOBP is formed by use of a physical bar ridge filter, and the PDD data of the SOBP, which are measured by the 3D water phantom, are registered in the proton treatment planning system. Therefore, the broad beam irradiation with a single field is highly robust for the dose uniformity in the tumor. On the other hand, the scanning irradiation method was used in one institute in this survey, and we consider that the robustness of the dose distribution at this institute was lower than that at the four institutions using the broad beam irradiation method.

Verification of the range measurement of each facility is very important, but it cannot be carried out with our group's verification tool at present. In many facilities offering proton and carbon beam therapies in Japan, the polybinary tissue model is used as the CT calibration method for WEL conversion [30]. In this study, we implemented a treatment plan for the liver phantom and we calculated the proton range. The average path length between the phantom surface and the radiation isocenter for the setup at each institute was 80.8(±1.4) mmWEL (phantom design value: 80.5 mmWEL = 77 mm (water) + 3 mm (acrylic) = 77 mmWEL + 3 mm * 1.16). We think that the CT calibration, which is an important factor in determination of the range accuracy of proton beams, is performed with high accuracy.

In this study, we considered that the accuracy of the absolute dose value irradiated to the tumor was one of the most important factors. The dose measurement with a radiochromic film shows a low value in the region of high stopping power of the proton beam. Therefore, we did not use the radiochromic film for measurement of dose distribution and we carried out dosimetric verification of only one axis of the OCR at the depth of the SOBP center using the air-filled ionization chamber with a small effect from stopping power. In addition, we did not calculate gamma index value and distance-to-agreement value for the evaluation of the calculated dose and the measured dose. We would like to consider verifications of 2-dimensional and 3-dimensional dose distributions with reference to the paper by Taylor et al. [10]. Recently, Lewis et al. [11] reported an anthropomorphic pediatric spine phantom designed for credentialing clinical trials of proton beam therapy. Similarly, it is possible to carry out dosimetric verification of the proton beam in a heterogeneous material using our designed liver phantom, with the installed rib phantom of high mass density.

In liver proton beam therapy, tumor positioning is performed by matching of bone or using bone and diaphragm in fluoroscopic images from two directions. In addition, management for respiratory motion of the tumor is important in liver proton beam therapy for liver [11,31–33]. Therefore, the proton beam irradiation method synchronized with the respiratory cycle was used for liver proton beam therapy in all the surveyed institutions. In our verification for JCOG1315C, we concluded that the quality of dose irradiation in positioning and respiratory movement of the tumor was assured by good implementation of quality control at each institution.

In summary, we designed the liver phantom and developed a dosimetric verification system for liver proton beam therapy in the JCOG1315C clinical trial. Credentialing in the clinical trial of proton beam therapy was performed for all (five) participating institutions. As a result of this visiting dosimetric survey and a dummy run (not described in this manuscript) for the JCOG1315C clinical trial performed by a proton treatment planning with CT images of liver, the clinical trial with integration of the institutions could be initiated. In the future, more institutions are expected to participate in the JCOG1315C clinical trial, and we will need to perform dosimetric verifications for new proton beam therapy systems of other manufacturers. It may be necessary to change from the visiting survey to a postal survey as the number of institutions participating in the JCOG1315C clinical trial increases.

## Declaration of Competing Interest

There are no conflicts of interest of disclose.

## Acknowledgments

We would like to thank the medical physicists and the staff of the institutions who helped us during the visiting survey. We would also like to thank the members of the JCOG Radiation Therapy Study Group, Medical Physics Working Group and Radiotherapy Committee for suggestions. This study was supported in part by the National Cancer Center Research and Development Fund (25-B-4, 28-A-14, 29-A-3 and 31-A-17) and the Japan Agency for Medical Research and Development (AMED Grant Number 18ck0106210 and 19ck0106485).

## Appendix A. Supplementary data

Supplementary data to this article can be found online at https://doi.org/10.1016/j.radonc.2019.06.005.

## References

[1] Wilson RR. Radiological use of fast protons. Radiology 1946;47:487–91.
[2] Tobias CA, Anger HO, Lawrence JH. Radiological use of high energy deuterons and alpha particles. Am J Roentgenol Radium Ther Nucl Med 1952;67:1–27.
[3] Lawrence JH, Tobias CA, Born JL, McCombs RK, Roberts JE, Anger HO, et al. Pituitary irradiation with high-energy proton beams: a preliminary report. Cancer Res 1958;18:121–34.
[4] Chu W, Ludewigt B, Renner T. Instrumentation for treatment of cancer using proton and light – ion beams. Rev Sci Instrum 1993;64:2055–122.
[5] https://www.ptcog.ch/index.php/facilities-in-operation.
[6] Kanai T, Kawachi K, Kumamoto Y, Ogawa H, Yamada T, Matsuzawa H, et al. Spot scanning system for proton radiotherapy. Med Phys 1980;7:365–9.
[7] Pedoroni E, Bacher R, Blattmann H, Bohringer T, Coray A, Lomax A, et al. The 200-MeV proton therapy project at the Paul Scherrer Institute: conceptual design and practical realization. Med Phys 1995;22:37–53.
[8] Lomax A. Intensity modulation methods for proton radiotherapy. Phys Med Biol 1999;44:185–205.
[9] Lomax A, Bohringer T, Coray A, Egger E, Goitein G, Grossmann M, et al. Intensity modulated proton therapy: a clinical example. Med Phys 2001;28:317–24.
[10] Taylor PA, Kry SF, Alvarez P, Keith T, Lujano C, Hernandez N, et al. Results from the imaging and radiation oncology core Houston's anthropomorphic phantoms used for proton therapy clinical trial credentialing. Int J Radiation Oncol Biol Phys 2016;95:242–8.
[11] Lewis DJ, Taylor PA, Followill DS, Sahoo N, Mahaja A, Stingo FC, et al. A new anthropomorphic pediatric spine phantom for proton therapy clinical trial credentialing. Int J Particle Ther 2018;4:20–7.
[12] http://www.jcog.jp/en/trials/index.html.
[13] Nishio T, Kunieda E, Shirato H, Ishikura S, Onishi H, Tateoka K, et al. Dosimetric verification in participating institutions in a stereotactic body radiotherapy trial for stage I non-small cell lung cancer: Japan clinical oncology group trial (JCOG0403). Phys Med Biol 2006;51:5409–17.
[14] Nishio T, Shirato H, Ishikawa M, Miyabe Y, Kito S, Narita Y, et al. Design, development of water tank-type lung phantom and dosimetric verification in institutions participating in a phase I study of stereotactic body radiation therapy in patients with T2N0M0 non-small cell lung cancer: Japan Clinical Oncology Group trial (JCOG0702). J Radiat Res 2014;55:600–7.
[15] Hatanaka S, Miyabe Y, Tohyama N, Kumazaki Y, Kurooka M, Okamoto H, et al. Dose calculation accuracies in whole breast radiotherapy treatment planning: a multi-institutional study. Radiol Phys Technol 2015;8:200–8.
[16] Nakamura M, Minemura T, Ishikura S, Nishio T, Narita Y, Nishimura Y. An on-site audit system for dosimetry credentialing of intensity-modulated radiotherapy in Japanese Clinical Oncology Group (JCOG) clinical trials. Phys Med 2016;32:987–91.
[17] Kawahara D, Ozawa S, Kimura T, Saito A, Nishio T, Nakashima T, et al. Marginal prescription equivalent to the isocenter prescription in lung stereotactic body radiotherapy: preliminary study for Japan Clinical Oncology Group trial (JCOG1408). J Radiat Res 2017;58:149–54.
[18] Okamoto H, Minemura T, Nakamura M, Mizuno H, Tohyama N, Nishio T, et al. Establishment of postal audit system in intensity-modulated radiotherapy by radiophotoluminescent glass dosimeters and a radiochromic film. Phys Med 2018;48:119–26.
[19] Okamoto H, Murakami N, Carvajal CC, Miura Y, Wakita A, Nakamura S, et al. Positional uncertainty of vaginal cuff and feasibility of implementing portable bladder scanner in postoperative cervical cancer patients. Phys Med 2018;45:1–5.
[20] https://upload.umin.ac.jp/cgi-open-bin/ctr_e/ctr_view.cgi?recptno=R000031842.
[21] Kirby D, Green S, Palmans H, Hugtenburg R, Wojnecki C, Parker D. LET dependence of GafChromic films and an ion chamber in low-energy proton dosimetry. Phys Med Biol 2010;55:417–33.
[22] Yeo IJ, Teran A, Ghebremedhin A, Johnson M, Patyal B. Radiographic film dosimetry of proton beams for depth-dose constancy check and beam profile measurement. J Appl Clin Med Phys 2015;16:318–28.
[23] Mizuno H, Kanai T, Kusano Y, et al. Feasibility study of glass dosimeter postal dosimetry audit of high-energy radiotherapy photon beams. Radiother Oncol 2008;86:258–63.
[24] Mizuno H, Fukumura A, Fukahori M, et al. Application of a radiophotoluminescent glass dosimeter to nonreference condition dosimetry in the postal dose audit system. Med Phys 2014;41:112104.
[25] Standard Dosimetry of Absorbed Dose to Water in External Beam Radiotherapy (Standard Dosimetry 12). Japan Society of Medical Physics; 2012 (in Japanese).
[26] Absorbed Dose Determination in External Beam Radiotherapy: An International Code of Practice for Dosimetry Based on Standards of Absorbed Dose to Water. Vienna: IAEA International Atomic Energy Agency; 2000.
[27] Kanehira T, Matsuura T, Takao S, Matsuzaki Y, Fujii T, Ito YM, et al. Impact of real-time image gating on spot scanning proton therapy for lung tumors: a simulation study. Int J Radiat Oncol Bio Phys 2017;97:173–81.
[28] Nishioka K, Prayongrat A, Ono K, Onodera S, Hashimoto T, Katoh N, et al. Prospective study to evaluate the safety of the world-first spot-scanning dedicated, small 360-degree gantry, synchrotron-based proton beam therapy system. J Radiat Res 2018;59:i63–71.
[29] https://www.jastro.or.jp/guideline/ (in Japanese).
[30] Kanematsu N, Matsufuji N, Kohno R, Minohara S, Kanai T. A CT calibration method based on the polybinary tissue model for radiotherapy treatment planning. Phys Med Biol 2003;48:1054–64.
[31] Knopf AC, Hong TS, Lomax A. Scanned proton radiotherapy for mobile targets-the effectiveness of re-scanning in the context of different treatment planning approaches and for different motion characteristics. Phys Med Biol 2011;56:7257–71.
[32] Bematowicz K, Lomax AJ, Knopf A. Comparative study of layered and volumetric rescanning for different scanning speeds of proton beam in liver patients. Phys Med Biol 2013;58:7905–20.
[33] Zhang Y, Knopf A, Tanner C, Lomax AJ. Online image guided tumour tracking with scanned proton beams: a comprehensive simulation study. Phys Med Biol 2014;59:7793–817.